Biochimica et Biophysica Acta, 934 (1988) 329–347
Elsevier

BBA 42811

Flash-induced H^+ binding by bacterial photosynthetic reaction centers: influences of the redox states of the acceptor quinones and primary donor

Péter Maróti * and Colin A. Wraight

Department of Physiology and Biophysics and Department of Plant Biology, University of Illinois, Urbana, IL (U.S.A.)

(Received 21 December 1987)

Key words: Bacterial photosynthesis; Reaction center; Proton binding; Quinone; (*Rb. sphaeroides*)

The flash-induced proton-binding behavior of reaction centers from *Rhodobacter sphaeroides* was examined, over a wide range of pH, as a function of the one-electron redox states of the acceptor quinones (Q_A/Q_A^- and Q_B/Q_B^-) and the primary donor (P^+/P). Below about pH 9, the P^+Q^- states ($P^+Q_A^-$ and $P^+Q_B^-$), generated in the absence of exogenous electron donor to P^+, fail to take up protons stoichiometrically, as established in the previous paper (Maróti, P. and Wraight, C.A. (1988) Biochim. Biophys. Acta 934, 314–328). When P^+ is rereduced by a donor, to yield the state PQ^-, proton binding is enhanced in this lower pH range. In the case of Q_B-reconstituted reaction centers, the net proton binding stoichiometry (H^+/P^+) for PQ_B^- is about 0.85, between pH 7 and pH 9, approaching the stoichiometric value expected for a pH-dependent redox midpoint potential of Q_B/Q_B^-. The shortfall from $H^+/P^+ = 1.0$ can be accounted for by the involvement of four protonatable groups with different pK values depending on the redox state of Q_B. The pK shifts vary from 0.3 to 1.5 pH units, with the lower pK groups exhibiting the smaller pK shifts. The enhancement of proton binding, associated with the rereduction of P^+, is interpreted as a response of the same groups to the redox state of P^+/P, with the lower pK groups exhibiting the largest pK shifts – up to 1.0 pH unit. A similar general behavior is seen for reaction centers lacking Q_B, or in the presence of terbutryn, a competitive inhibitor of Q_B-binding. Quantitatively, the rereduction of P^+ does not restore such high levels of H^+ binding for PQ_A^- or PQ_A^- / + terbutryn ($H^+/P^+ \leqslant 0.5$ at all pH values), but the behavior can be similarly accounted for by four protonatable groups that are somewhat less responsive to the redox states of Q_A and P. The pK values for the three different acceptor configurations (Q_B, Q_A and Q_A/ + terbutryn) are similar but not identical, and depend on the redox states of the primary donor and the acceptor quinones, and on the occupancy of the Q_B-binding site. The pK values are discussed in terms of possible structural determinants of the quinone binding sites. The data define protonation networks for the reaction center states PQ, P^+Q^- and PQ^-, and allow one to deduce the properties of a fourth state: P^+Q. The derived pK values predict the occurrence of H^+ release from the state P^+Q, at low pH, and this was confirmed by using ferricyanide to reoxidize Q^- following a flash to generate P^+Q. The

---

* Permanent address: Institute of Biophysics, József Attila University, Szeged, Egyetem u.2., Hungary.

Abbreviations: CAPS, 3-[cyclohexylamino]-1-propanesulfonic acid; Bistris, 2-[bis(2-hydroxyethyl)amino]-2-(hydroxymethyl)propane-1,3-diol; Bistris propane, 1,3-bis[tris(hydroxymethyl)methylamino]propane; DAD, diaminodurene; Hepes, 4-(2-hydroxyethyl)-1-piperazineethanesulfonic acid; Mes, 4-morpholineethanesulfonic acid; Mops, 4-morpholinepropanesulfonic acid; Q, Q_A and/or Q_B; Q-10, ubiquinone-50; RC, reaction center; Triton, Triton X-100.

Correspondence: C.A. Wraight, Department of Plant Biology, University of Illinois, 289 Morrill Hall, 505 S. Goodwin Avenue, Urbana, IL 61801, U.S.A.

proposed protonation scheme allows the calculation of the pH dependence of the one-electron transfer equilibrium between $P^+Q_A^-Q_B$ and $P^+Q_AQ_B^-$. This agrees well with the measured value, derived from the kinetics of charge recombination. However, the pK changes, derived from the enhanced proton binding that accompanies rereduction of P^+, give rise to a substantial discrepancy between the calculated and measured values for the $PQ_A^-Q_B \leftrightarrow PQ_AQ_B^-$ equilibrium. The pH dependences of the redox midpoint potentials (E_m) of Q_A/Q_A^-, Q_B/Q_B^- and P^+/P are also calculated. Good agreement between calculated and measured values is obtained for P^+/P, and between the calculated value for Q_B/Q_B^- and that expected from studies on chromatophores. However, the calculated pH dependence of $E_m(Q_A/Q_A^-)$ is at variance with that measured in isolated reaction centers or chromatophores. These discrepancies are discussed but not resolved.

Introduction

In the preceding paper [1], we described the flash-induced H^+ binding by isolated reaction centers from *Rhodobacter sphaeroides,* in the absence of an electron donor to P^+. Using two entirely independent methods, we observed that the proton uptake at high pH values (pH > 9) follows the behaviour expected from the equilibrium redox properties of the acceptor quinones, but is anomalously small at lower pH values (pH < 9). An earlier study on the pattern of H^+ binding in a series of flashes, in the presence of an electron donor to P^+, appeared to be roughly consistent with these observations in the absence of donor [2]. Thus, at pH values below 8.5 significant oscillations, of period 2, were observed, reflecting low uptake on the first flash. Between pH 6.5 and pH 8, proton binding stoichiometries (H^+/P^+) of 0.4–0.6 and 1.6–1.4 were observed on the first and second flashes, respectively. Below pH 6.5 the oscillations became more marked, approaching a pattern of 0, 2, 0, 2, etc. At pH values above 8 the oscillations diminished and, by pH 9, roughly equal H^+ binding stoichiometries were observed on each flash.

The state of the reaction center (RC) after a single flash in the presence of donor (PQ^-) is at least roughly equivalent to that formed in equilibrium redox titrations of the acceptor quinones, which indicate that RCs bind one proton upon reduction of Q_A, or Q_B, to the semiquinone state [3–5]. We, therefore, considered that the failure to observe stoichiometric proton binding after a single flash might indicate a kinetic block [6]. In the case of mitochondrial cytochrome *c*, oxidation at high pH is followed by slow proton unbinding, which is linked to a conformational change requiring many seconds to complete [7–9]. However, attempts to test this model did not reveal any slow proton uptake, by RCs, in the seconds-to-minutes time range. We, therefore, began to reexamine the H^+ binding stoichiometries for RCs in the presence of donor. Our current work confirms a complex pH-dependence of the proton binding stoichiometry, but with some quantitative differences compared with earlier results. In this paper we describe the application of spectrophotometric and conductimetric methods [1] to establish the proton binding stoichiometries, in a series of flashes, for RCs in the presence of electron donors to P^+. The observed stoichiometry is sensitive to pH and to the functional state of the acceptor quinone complex, i.e., whether secondary quinone (Q_B) is functioning or only the primary quinone (Q_A) is active, and whether inhibitors of Q_A to Q_B electron transport are present. In contrast to our earlier measurements, we now find that, between pH 7 and pH 9.5, in the presence of donors, the proton binding stoichiometry (H^+/P^+) is in excess of 0.8, but less than 1.0, when Q_B is functional. The pH dependences of the proton binding stoichiometry are also described for RCs lacking Q_B or in the presence of terbutryn, an inhibitor of Q_B activity. The results are discussed in terms of multiple protonation equilibria under the influence of the redox states of the primary donor, P^+/P, and of the acceptor quinones, Q/Q^-.

Materials and Methods

The preparation of RCs from *Rb. sphaeroides,* strains R26 and Ga, was performed as previously described [1,2]. Measurements of H^+ binding and

release, by conductimetric and spectrophotometric methods, were also as described in the preceding paper [1]. Routinely, samples for spectroscopic assay contained 0.5–2 μM RCs in 100 mM NaCl, 0.03–0.06% Triton X-100, but some studies were done at low salt (10 mM) for comparison with the conductance measurements. The effect of replacing the Triton X-100 by 0.05% LDAO (lauryldimethylamine *N*-oxide/Ammonyx LO, a gift of Onyx Chemical Corp., Division of Millimaster, NJ) was also examined. Conductance samples contained no salt but were in 10 mM buffer, 0.03–0.06% Triton X-100.

Because of the long lifetime of the semiquinone states of the RC in the presence of donor, i.e., PQ_A^- and PQ_B^-, special care was taken, in the spectrophotometric measurements, to minimize the integrated light exposure of the samples with donor. Samples were dark adapted for 15 min with no measuring beam on, and shutters over the measuring beam were opened only 2 s before the actinic flash sequence. Simultaneous measurements at two wavelengths were sometimes recorded, but the additional measuring beam intensity was considered a possible source of activation. The sufficiency of the normal dark-adaptation procedure was checked by comparison with 'absolute' dark adaptation of the samples, achieved as follows. A large volume of sample, lacking only buffer, was made up in the dark. One sample was taken to set the photomultiplier voltages and the slit widths for two monitoring wavelengths, and to determine appropriate gains of the amplifier. The two wavelengths were selected for measurement of the pH-indicator and semiquinone absorbance changes. A second aliquot was then taken for assay of the pH-indicator response, at an appropriate wavelength (often at about 587 nm), followed by acid calibration. A separate sample, with buffer added, was used to determine the background response, followed by acid calibration to check the extent of buffering. A fourth sample was used to monitor the semiquinone oscillations, at 450 nm. This, too, was buffered to eliminate any H^+ responses of the pH-indicator at this wavelength. All H^+ binding data reported as 'net' are corrected for non-bufferable, background responses.

In addition to the external H^+ calibration methods, described in Ref. 1, data were frequently expressed on the basis of internal calibration, using a steady-state proton binding stoichiometry of 1.0 H^+ per RC, which assumes 100% turnover of the RC on each flash. In fact, the electron sharing between $Q_A^-Q_B$ and $Q_AQ_B^-$ leads to a failure of turnover of a small proportion of RCs, equal to $1/(1 + K_2)$, where K_2 is the equilibrium constant for this electron-transfer equilibrium [10]. Below about pH 9, $10 < K_2 < 20$, and the error is less than 10% [2,10–12]. At higher pH, this internal normalization procedure fails and external calibration becomes essential.

In some experiments it was desired to resolve the rise kinetics of the proton binding on the first flash, but still to be able to record the extent of binding in a series of flashes for purposes of internal calibration. In such cases, the amplifier output was stored in a Biomation 805 transient recorder with a split time base. The trace could then be transferred asynchronously to the usual file format of the LSI 11/73-based signal averager [12]. In a similar manner, internal calibration could also be applied to Q_B-depleted RCs, by giving one flash for assay of the Q_A-related H^+ binding, followed quickly by addition of excess ubiquinone and administration of a series of flashes.

Donors to the RC were added from stock solutions, as follows: horse heart cytochrome *c* (Type III; Sigma Chemicals, St. Louis), 1–3 mM stock solution in water, reduced by stoichiometric titration with sodium dithionite, 8–32 μM final concentration; ferrocene (Sigma) and acetylferrocene (Sigma), 50 mM stock solution in ethanol, 5–250 μM final concentration; DAD (diaminodurene, 2,3,5,6-tetramethyl-*p*-phenylenediamine), 10 mM stock solution in dilute HCl and then neutralized, 100–500 μM final concentration; TMPD (*N,N,N',N'*-tetramethyl-*p*-phenylenediamine), 10 mM stock solution in water, 100 μM final concentration; hexammineruthenium(III) chloride (Aldrich Chemicals), 0.1 M stock solution in water, 100–800 μM final concentration: Ru^{III} was reduced to Ru^{II}, in the cuvette, by titration to a suitable redox potential, i.e., $E_h \approx 130$ mV at pH < 7.

Redox titrations were performed as described previously [2–5]. For titrations of Q_A/Q_A^-, mediators included: 20 μM each of 1,4-naphthoquinone,

1,2-naphthoquinone, 2-hydroxy-1,4-naphthoquinone, 5-hydroxy-1,4-naphthoquinone and duroquinone; 1–5 μM pyocyanine and ethylpyocyanine; 0.5–1 μM phenazinemethosulfate and phenazineethosulfate (PMS and PES). In some experiments, one or other of the following were also present (20 μM): DAD, TMPD, indigo carmine (indigo trisulfonate) and ferric EDTA. For titrations of P^+/P, the mediators were 20 μM DAD or TMPD, 20 μM benzoquinone, and potassium ferricyanide added as titrant.

Results

Proton binding by Q_B-reconstituted reaction centers: characterization of ferrocene as a suitable electron donor

In our earlier studies [2], cytochrome *c* was used as the donor to P^+ because it is known to be a pure electron redox couple at pH values below a p*K* on the oxidized form, at pH 9.1 [9]. However, this required the rather precise definition of an isosbestic wavelength for cytochrome oxidation, to

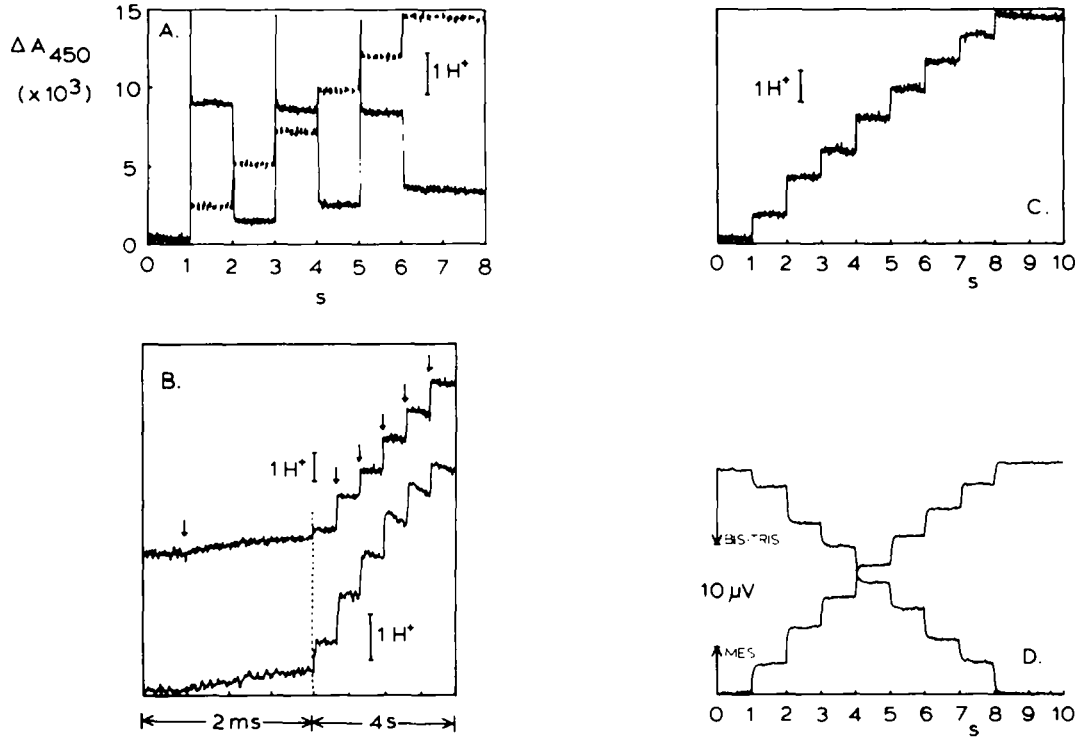

Fig. 1. Comparison of donors, ionic conditions and assay methods for flash-induced proton uptake by reaction centers (R26). Left panels: Proton binding in the presence of salt, with ferrocene as donor. Conditions: 1.4 μM reaction centers in 100 mM NaCl, 0.03% Triton X-100, 20 μM Q-10, 100 μM ferrocene, 0.6 mM potassium ferrocyanide, 40 μM pH indicator. (A) Parallel measurements of H^+ binding and semiquinone absorbance changes in absolutely dark-adapted samples, at pH 5.0, with 40 μM bromocresol green; (- - - - - -) net proton binding signal measured as the difference between the signal at 586 nm with and without 10 mM malate buffer; (———) semiquinone signal measured at 450 nm, with buffer present. (B) Net proton binding signals. Top: pH 7.60 (40 μM bromothymol blue/±10 mM Hepes buffer). Bottom: pH 9.25 (40 μM thymol blue/±10 mM Bistris propane buffer). Traces recorded on split time base, as indicated. Actinic flashes were administered at the arrows. Right panels: Proton binding measurements at pH 6.36, in low salt, with cytochrome *c* as donor. (C) Net proton binding measured with indicator, at 560 nm, as described in part A. Conditions: 0.74 μM reaction centers in 10 mM NaCl (pH 6.36), 0.03% Triton X-100, 20 μM Q-10, 16 μM cytochrome *c*, 10 μM 1,4-naphthoquinone, 40 μM bromocresol purple, ±10 mM Mes buffer. (D) Conductance changes in a flash series. Conditions: 1.3 μM reaction centers, 10 mM buffer (pH 6.36), 0.03% Triton X-100, 20 μM Q-10, 16 μM cytochrome *c*, 10 μM 1,4-naphthoquinone. Upward trace: Mes buffer, $G = (1213\ \Omega)^{-1}$; downward trace: Bistris buffer, $G = (1042\ \Omega)^{-1}$; vertical scale arrows indicate 10 μV for each buffer system, and the direction of the flash-induced change (an upward deflection indicates a conductance increase). The traces are shown without correction for the flash-related heart artifact, which was quite small. The H^+/P^+ values (calculated as in Ref. 1) are given in Table I.

minimize the background signal which must be subtracted to reveal the net H^+ binding signal of the pH indicator dye. We, therefore, screened several redox agents to find a donor with better spectral characteristics. The preference for an electron donor, rather than a hydrogen atom couple, limited the field considerably, but we found that ferrocene was particularly well suited. Although of rather high midpoint potential ($E_m = 524$ mV in dimethylformamide, 50 mM tetrabutylammoniumtetrafluoroborate [13], and 437 mV in aqueous detergent, pH 7.0 [14]), ferrocene is sufficiently soluble to permit concentrations up to 300 μM, i.e., in great excess over that of the RCs. Potassium ferrocyanide was also routinely added, in excess (0.5–1 mM), to rereduce the oxidized ferrocene (ferricinium). The rereduction of P^+ by ferrocene was found to be second order, with a rate constant of $(4 \pm 2) \cdot 10^6\ M^{-1} \cdot s^{-1}$, from pH 6 to pH 10 (not shown). The absorbance and oxidized-minus-reduced difference spectra of ferrocene are negligible in the visible region, including the 450 nm region, relevant to semiquinone measurements, and the 540–600 nm range useful for most pH indicators.

Fig. 1A and B shows several traces of the net proton binding signal (unbuffered-minus-buffered dye response), with ferrocene as donor and using various pH indicator dyes, to cover a range of pH values. It is clear, simply from visual inspection of the depth of the oscillations, that the H^+/P^+ stoichiometry on the first flash is significantly greater than the value of 0.5 reported earlier [2]. Indeed, both external and internal calibrations show the stoichiometry to be 0.85 ± 0.1 over much of the pH range, up to pH 9.5. The smaller oscillations, observed in the present work, could indicate the existence of some Q_B^- prior to the flash sequence. However, this was not the case, as parallel measurement of the oscillating Q_B^- and H^+ binding signals, on fully dark-adapted samples (e.g., Fig. 1A), showed the amplitude of the 450 nm absorbance change to be as expected from the extinction coefficient of Q_B^- [15]. Even in the worst cases, we could account for no more than 12% Q_B^- prior to the flash sequence, and the amount was generally much less.

In order to examine the discrepancy between the present measurements and those reported earlier [2], we returned to the original measuring conditions, as well as trying many variations of donor, dye and monitoring techniques. Some of

TABLE I

COMPARISON OF H^+-BINDING WITH DIFFERENT DONORS, METHODS AND DYES

Δ1 through Δ4 are the H^+/P^+ stoichiometries on each of the first four flashes, delivered to a dark-adapted sample of reaction centers in the presence of the donor indicated in column 1. The stoichiometries are normalized to a steady-state yield of 1.0 averaged over six flashes. Methods: spectrophotometric (Spect.) and conductimetric (Conduct.) assays. pH indicator dyes used: chlorophenol red and bromocresol purple.

Donor	pH	H^+-stoichiometry (H^+/P^+)				Method	NaCl (mM)
		Δ1	Δ2	Δ3	Δ4		
Ferrocene [a]	6.28	0.77	1.25	0.83	1.16	Spect.	100
Cytochrome	6.45	0.77	1.27	0.76	1.20	Spect.	100
$Ru^{II}(NH_3)_6$	6.26	0.81 [b]	1.20	0.85	1.14	Spect.	10
Cytochrome [c]	6.31	0.79	1.21	0.85	1.07	Spect.	10
Cytochrome [d]	6.32	0.75	1.22	0.91	1.13	Conduct.	– [e]

[a] Average of two independent measurements.

[b] Stoichiometries are corrected for H^+-release (0.21 H^+/P^+) associated with oxidation of hexammineruthenium(II) as donor (see text).

[c] Average of three independent measurements; S.E.M. ≤ 0.05.

[d] Average of three independent measurements; S.E.M. ≤ 0.03.

[e] No NaCl, but 10 mM Bistris or Mes, in two separate samples (see Materials and Methods).

these experiences will be detailed here as they may provide useful guidance for further research in this area.

Proton binding by Q_B-reconstituted reaction centers: comparison of ferrocene and cytochrome c as electron donors

Fig. 1C and D and Table I compare the proton binding pattern observed, in a narrow pH range (pH 6.2–6.5), with three different donors – ferrocene, cytochrome *c* and hexammineruthenium (II) – and examine the effect of salt concentration. The optical and conductimetric methods of detection are also compared. These results show cytochrome *c* and ferrocene to be essentially equivalent as donors and, together with data over a wide range of pH, do not support our previous measurements with cytochrome *c*, which indicated a dramatic drop-off of first-flash proton uptake below about pH 6.3 [2]. No marked dependence on salt concentration was evident in this pH range. An advantage of cytochrome *c* as donor is that the effective turnover of the RCs can be easily monitored for each flash, through the amplitude of the cytochrome oxidation signal at 550 nm. This allows for correction for any failure in turnover of the RCs due, e.g., to the presence of Q_A^-, arising from lack of reconstitution of Q_B or from electron sharing between $Q_A^-Q_B$ and $Q_AQ_B^-$ [2,11,16]. At pH values below 10, however, the difference is small (less than 10%), and calculation of the data of Table I as H^+/cytochrome c^+ did not alter the relative stoichiometries. For convenience of comparison between various donors, therefore, stoichiometries were routinely based on internal calibration (see below), or an external acid calibrations using the total RC content of the sample to express the ratio H^+/P^+.

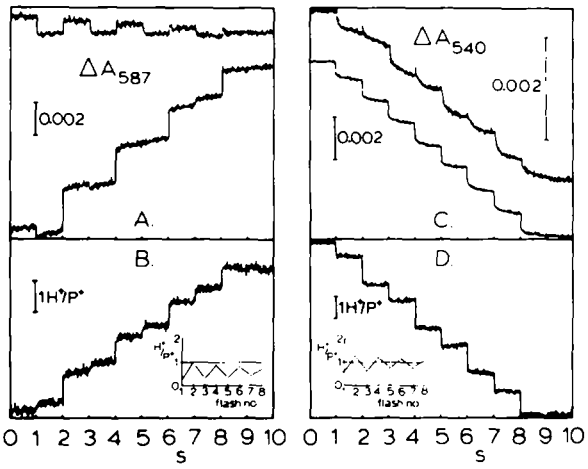

Fig. 2. Absorbance changes and net proton binding signals. Conditions: 0.95 μM reaction centers (Ga), 10 mM NaCl, pH 5.84, 0.03% Triton X-100, 20 μM Q-10, 40 μM pH indicator, donor as given. Left panels: Measurements with hexammineruthenium(II) as donor (0.8 mM hexammineruthenium(III/II) chloride, $E_h \approx 130$ mV) and bromocresol purple as pH indicator. (A) Absorbance changes, at 587 nm, in the presence (top) and absence (bottom) of buffer (4 mM succinate/4 mM Mes, pH 5.84). (B) Net proton binding signal derived from the traces of part A (unbuffered-minus-buffered). Inset: flash pattern of net proton binding determined by external calibration (see Materials and Methods) – the low apparent H^+/P^+ stoichiometry (average, $H^+/P^+ \approx 0.61$) arises from H^+ release by exogenous donor (see text). Right panels: Measurements with cytochrome *c* (16 μM) as donor and methyl red as pH indicator. (C) Absorbance changes, at 540 nm, in the presence (top) and absence (bottom) of buffer (as for part A) – note different vertical scales. The signal in the presence of buffer includes two components – an oscillating signal due to electrochromic responses to Q_B^-, and a stepwise decrease in absorbance due to cytochrome oxidation (the measuring wavelength was not quite isosbestic). (D) Net proton binding signal derived from the traces of part C (unbuffered-minus-buffered). Inset: flash pattern of net proton binding determined by external calibration (average, $H^+/P^+ \approx 0.94$).

Non-bufferable (electrochromic) responses of pH indicator dyes

In spite of the good agreement between the data with two donor systems, we were concerned that the spectrophotometric method is reliant on subtraction of background signals which are, themselves, oscillating (Fig. 2). At most wavelengths in the region suitable for monitoring the pH indicators, the electrochromic effect of Q_B^- on the endogenous chromophores of the RC gives rise to oscillations in phase with the semiquinone oscillations of the two-electron gate [17]. Furthermore, almost all pH indicator dyes tested with isolated RCs exhibited significant oscillating signals in the presence of sufficient buffer to eliminate any direct response due to proton binding. These signals presumably arise from an electrochromic influence of the Q_B^- charge state of the RC on dye molecules directly adsorbed to the complex. The signal is

hardly affected by the level of detergent present, but is diminished by sufficiently high ionic strength. Under our normal conditions of assay (i.e., 100 mM NaCl), the buffered signal of most pH indicators is small, but not absent, and care must still be taken that addition of the buffer does not significantly alter the amplitude of this signal. The electrochromic influences of Q_B^- on the native pigments of the RC are also somewhat ionic-strength dependent (not shown).

With these precautions in mind, we have not observed any significant differences in proton binding stoichiometries in low (10 mM) or high (100 mM) salt, in the presence of donor, at pH values below about 9 (Table I). The effects of higher ionic strengths, especially at pH values above 9, will be described elsewhere, but are consistent with an ionic screening effect on the highest pK values governing proton uptake (see below). The buffered signal of the pH indicator dyes is almost absent in chromatophores [18], or with RCs incorporated into phospholipid vesicles (not shown), suggesting that the effect in solubilized RCs arises from a population of dye molecules adsorbed to the hydrophobic 'sides' of the complex. For bromocresol purple, this is supported by the blue shift of the center wavelength of the electrochromic response (approx. 575 nm), compared to the peak wavelength of the absorbance spectrum for bulk phase indicator (approx. 585 nm) (Fig. 3).

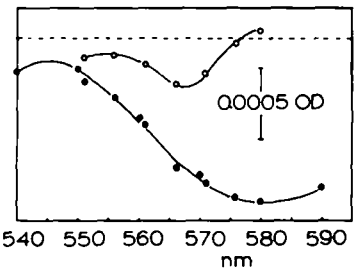

Fig. 3. Spectra of background absorbance changes associated with the presence of pH indicator. Conditions: 0.6 μM reaction centers (R26), 10 mM NaCl (pH 6.4), 0.03% Triton X-100, 20 μM Q-10, 100 μM DAD. Absorbance change magnitudes calculated as: 1/2{Δ(flash 1)-minus-Δ(flash 2)}. ●, flash-induced absorbance spectrum in the presence of dye (40 μM bromocresol purple) and buffer (10 mM Mes, 8 mM Bistris); ○, (no dye)-minus-(dye + buffer) difference spectrum.

Conductance measurements of proton binding with cytochrome c as donor

The most striking characteristic of proton binding, during turnover of the acceptor quinones, is its oscillating nature, and the possibility that this feature might be artifactually imprinted on the data by an erroneous subtraction of the background signal, was hard to rule out. We, therefore, made some conductimetric measurements of H^+ uptake by RCs in the presence of donor. We have previously demonstrated a good agreement between the spectrophotometric and conductimetric methods for H^+ binding in the absence of donor [1]. Fig. 1D shows the conductance changes in a flash sequence, in the buffer pair: Mes and Bistris (pH 6.36), for RCs with cytochrome *c* as donor. The excellent signal-to-noise characteristics of the conductance method are evident in this figure. From these traces the H^+ binding can be calculated, as described [1], and the results are summarized in Table I. The agreement with the pH indicator measurements (see Fig. 1C) is good, and the pattern is, again, one of shallow, but distinct, oscillations with an H^+/P^+ ratio of about 0.8 on the first flash. There are no serious candidates for an artifactual source of oscillations in the conductance measurements (but see below), and the mere existence of the oscillatory pattern essentially dispells the possibility that the true proton stoichiometry on the first flash is 1.0, with apparent oscillations, in the spectrophotometric assay, arising from background subtraction artifacts.

Internal calibration and anomalies of proton release from hydrogen carriers

It is often a convenience, as well as a source of greater precision, to be able to use an internal calibration for measurement of hydrogen ion binding or release in biological systems, i.e., the flash stoichiometries are normalized to the value in the steady state. The requirement is that the steady-state stoichiometry be well defined, either by experiment or by incontrovertible logic. The latter is generally assumed in studies on flash-induced proton movements in chloroplasts [19,20], where the overall chemistry of water oxidation determines that the steady state proton release coupled to the reduction of a pure electron acceptor, such as ferricyanide or methyl viologen, is $H^+/e^- = 1.0$.

Similarly, the redox chemistry of ubiquinone, in solution, leads us to expect a steady-state uptake of 1.0 H^+ per electron when the donor to P^+ is an electron donor. However, when the redox chemistry of either the donor or the acceptor system is uncertain, this procedure can be misleading.

Fig. 4 shows H^+ binding data with three different donors. With TMPD as donor, at pH 5.6, H^+ binding was determined from measurements of conductance changes in a flash series, using the buffer pair: piperazine and succinate (see Ref. 1). The raw data indicated dramatic oscillations in ionic conductance (not shown) which translate into deep oscillations of H^+ binding (Fig. 4A). However, external calibration of the data clearly showed that the binding is substoichiometric, and averages only 0.22 H^+ bound per RC (Fig. 4A). Thus, the depth of the oscillations is only apparent. The shortfall from the expected 1.0 H^+ bound per electron is due to proton release from the oxidation of TMPD, and correction for this reveals proton binding oscillations similar to those obtained with other donors. The stoichiometry of proton release observed (0.78 H^+/e^-) is consistent with a pK of about 6.1 on the reduced form, i.e., TMPD/$TMPDH^+$, in reasonably good agreement with published values of 6.3–6.6 for the redox pK, determined under similar, but not identical, conditions [21]. Below this pK, the reduced form is largely protonated and oxidation of $TMPDH^+$ is accompanied by H^+ release ($TMPDH^+ \rightarrow TMPD^+ + H^+$). Above the p$K$ on the reduced form, oxidation results in the net gain of a positive charge ($TMPD \rightarrow TMPD^+$) with no proton release. The conductance method can detect this net, non-proton, ion production [1] but the calibration is less accurate because: (i) it is a secondary calculation that utilizes the H^+/P^+ ratio, (ii) the buffer-pair method is not applicable, so the heat artifact must be compensated for directly, by subtraction; and (ii) the conductance change can be specified only in terms of equivalents of some standard ion for which the specific conductance, or mobility, is well known. Using Cl^- for this purpose, we calculate that 0.11 'Cl^- equivalents' are produced per flash at pH 5.6.

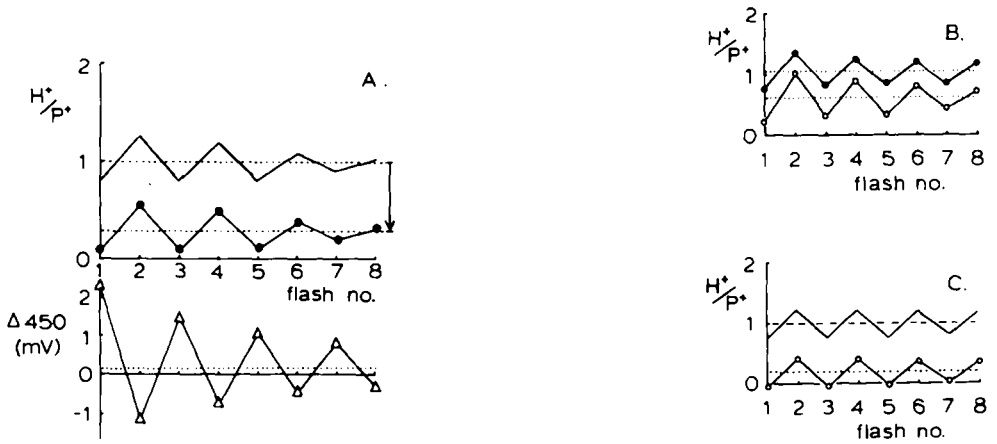

Fig. 4. Net H^+ oscillations observed with proton-linked donors. (A) Net proton binding with TMPD as donor, measured by the conductance method with the buffer pair, piperazine/succinate, as described in Ref. 1. Conditions: 0.86 μM reaction centers (Ga), 10 mM buffer (pH 5.58), 0.03% Triton X-100, 20 μM Q-10, 100 μM TMPD. Top: ●, net proton binding oscillations, calculated as described in Ref. 1; ———, H^+ oscillations off-set by 0.78 (arrow) to give an average $H^+/P^+ = 1.0$. Bottom: semiquinone signal changes, measured at 450 nm, determined simultaneously with the conductance measurement; ·····, steady-state absorbance change at 450 nm, due to TMPD oxidation. (B) Net proton binding with hexammineruthenium(II) as donor, measured optically at 588 nm. Conditions: 1.0 μM reaction centers (Ga), 10 mM NaCl, 0.03% Triton X-100, 20 μM Q-10, 40 μM bromocresol purple; ○, 0.8 mM hexammineruthenium(III/II) chloride, $E_h \approx 130$ mV (pH 5.83); ●, 0.2 mM hexammineruthenium(III/II) chloride, $E_h \approx 130$ mV (pH 6.69). ·····, average H^+/P^+ stoichiometries determined by external calibration = 0.62 at pH 5.83, and 1.04 at pH 6.69. (C) Net proton binding with DAD as donor, measured optically at 540 nm. Conditions: as for (B), except with 40 μM methyl red (pH 5.72); ○, 0.2 mM DAD, as donor; ———, H^+ oscillations off-set by 0.8 to give an average $H^+/P^+ \approx 1.0$.

Considering that the mobility of $TMPD^+$ is certainly lower than that of Cl^-, this small value is consistent with the calculated proton release that accompanies the oxidation of $TMPDH^+$, from which we would expect a net charge gain of 0.22, per turnover, in the form of $TMPD^+$ generated from TMPD.

Concomitant H^+ binding, by the RC, and release, from the exogenous donor, was also observed with hexammineruthenium(II) chloride (Figs. 2A and 4B) and with diaminodurene (DAD) (Fig. 4C) as donors. The former is expected to be a pure electron donor at all pH values [22], yielding a net proton binding by the RC of $1H^+/P^+$ in a flash sequence. However, at pH 5.88 the average proton binding stoichiometry was only 0.61 H^+/P^+, indicating the existence, at about pH 5.7, of a pK on the reduced form (Ru^{II}), so that a proton is released upon oxidation at acid pH. Since hexammineruthenium is well established as a non-protonated redox couple [22], this is presumably a property of a contaminating entity such as a reductant species derived from the dithionite or, possibly, pentaammineaquoruthenium ($Ru^{III/II}(NH_3)_6H_2O$), which might be formed by hydrolysis at low pH [23]. Although exhibiting useful spectroscopic properties, i.e., little absorbance in the visible range, ruthenium ammines are limited in utility, even at higher pH values, due to their rather low redox midpoint potentials ($E_m \approx 100$ mV, for hexammineruthenium [22,23]). The proton release observed with DAD as donor (approx. 0.8 H^+/e^- at pH 5.7; 0.6 at pH 6.3) is reasonably consistent with the somewhat conflicting and incomplete data, reported in the literature, for this complex redox agent (see Ref. 21).

In Fig. 2B, with cytochrome c as donor at pH 5.88, the average proton binding stoichiometry, by external calibration, was 0.94 H^+/P^+. This is certainly not due to proton release from oxidized cytochrome c, which is negligible at pH values below 8 [9]. It is, in fact, essentially identical to what is expected by taking into account the effect of the electron transfer equilibrium, K_2, between $Q_A^-Q_B$ and $Q_AQ_B^-$, on the average turnover of the RC [2,11]. However, this is more likely a fortuitous agreement than an accurate reflection of the precision of the proton binding data (compare Fig. 4B, with hexammineruthenium(II) as donor, at pH 6.69, where the average proton binding was 1.04 H^+/P^+)!

Under certain conditions, we encountered an unexpected result which can, in fact, contribute an 'artifactual' oscillation to the H^+ conductance change, albeit not one that is likely to confuse the real issue. At high pH, oxidized $TMPD^+$ directly oxidizes ubiquinol. Since ubiquinol is released from the reaction center in an oscillating pattern, its oxidation by $TMPD^+$ also oscillates, releasing protons into the medium predominantly on even flashes. The proton binding/release pattern, determined by the conductimetric method, at pH 10, closely followed the kinetics of TMPD oxidation and rereduction, measured at 570 nm (not shown). It has previously been shown that some oxidants, including ferricyanide [24] and $TMPD^+$ [25], can directly oxidize Q_A^- and, indirectly, Q_B^-. However, this was not evidenced in the oscillating Q_B^- signal, which was stable between flashes. Furthermore, the $TMPD^+$ signal after the first flash was quite stable compared to the rapid decay ($t_{1/2} <$ 0.3 s) after the second and subsequent flashes. Thus, the direct oxidation of semiquinone was a minor activity, here. Oxidized ferrocene was also able to slowly oxidize ubiquinol and showed some activity with the acceptor semiquinones (not shown). Since ferrocene was normally employed with an excess of ferrocyanide to rereduce the ferricinium, this was not generally a problem. Ferricyanide, which has been shown to oxidize Q_A^- directly at pH values below 6.5 [24], did not accumulate in sufficient quantities to reveal this activity.

pH dependence of proton binding by reaction centers in various states of acceptor quinone activity

Fig. 5 shows compilations of the first flash proton stoichiometries for RCs with three different acceptor configurations – Q_B reconstituted (Fig. 5A), plus terbutryn (Fig. 5C) and Q_B depleted (Fig. 5B). Between pH 5 and pH 10, data for Q_B-reconstituted RCs are plotted for both external and internal calibrations. At high pH (pH > 9.5), the steady-state level of Q_A^- is significant and the steady-state H^+-binding stoichiometry, expressed in terms of the total reaction center content, no longer approaches 1.0. Under these conditions, external calibration is essential. Also

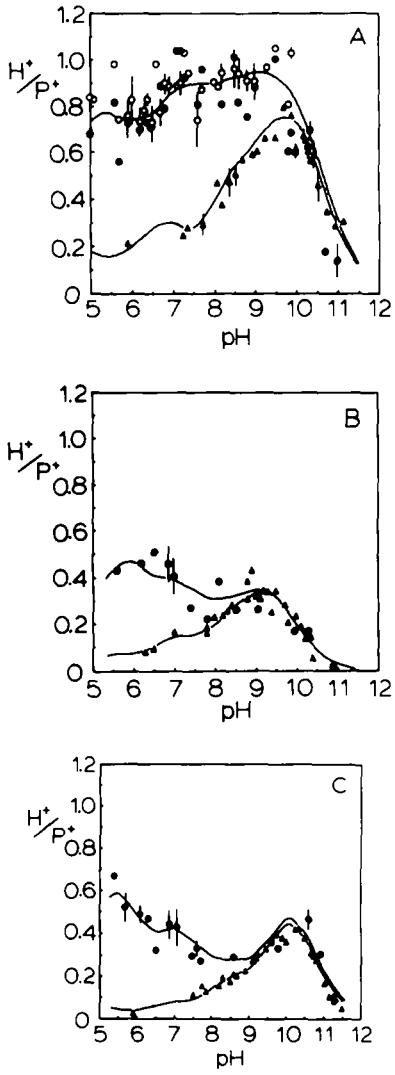

Fig. 5. Compiled data for net proton binding by reaction centers in various states of acceptor quinone activity. (A) Q_B-reconstituted. Conditions: 100 mM NaCl, 0.03% Triton X-100, 20 μM Q-10; spectrophotometric assay with various pH indicators. Circles: with exogenous donors (various, but mostly ferrocene or cytochrome *c*); ○, internal calibration with average $H^+/P^+ = 1.0$; ●, external calibration with standard HCl. Triangles: no exogenous donor; taken from Ref. 1, after averaging data over intervals of 0.05 pH. (B) Q_B-extracted. Conditions: as for A except no Q-10. External calibration only. (C) Terbutryn inhibited. Conditions: as for A, except plus 60 μM terbutryn. Lines are drawn according to the model described in the text, using Eqn. 1 and p*K* values summarized in Table II.

shown are data obtained in the absence of donor; these are taken from the previous paper [1] but, for clarity, the number of data points has been reduced by averaging over pH intervals of 0.05.

Above about pH 9, the data in the presence or absence of donor agree well, and seem to reflect the protonation behaviors of Q_A and Q_B expected from their equilibrium redox properties. At lower pH values, however, the proton binding is higher in the presence than in the absence of donor. This is especially noticeable when Q_B is present (Fig. 5A): between pH 7 and pH 9.5, in the presence of donor, the H^+-binding stoichiometry is greater than 0.8. However, the continued presence of shallow oscillations, in this pH range, strongly indicates that the first flash stoichiometry does not actually reach 1.0. When Q_B function is lacking, either through the addition of terbutryn (Fig. 5B) or by extraction of ubiquinone (Fig. 5C), the extent of proton binding is much lower and does not exceed 0.5 H^+ per RC at any pH value. Nevertheless, in both cases there is a marked enhancement of H^+ uptake at low pH, associated with the presence of a donor to P^+.

As a possible source of influence on the proton-binding stoichiometry, we compared the effect of LDAO, another commonly used detergent. LDAO is widely used for the isolation and purification of RCs, but it is often subsequently replaced for studies involving redox poising. We have routinely worked with Triton X-100 in the suspension medium. Fig. 6 shows the pH dependence of first flash proton binding by Q_B-active RCs in the presence of donor, in 100 mM NaCl and 0.03% LDAO. These data are clearly very similar to those of Fig. 5A, obtained with Triton

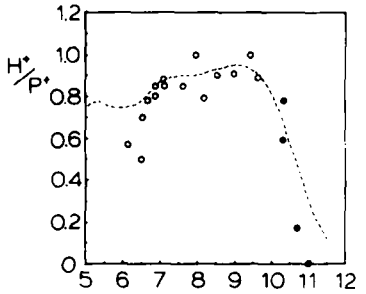

Fig. 6. Net proton binding by Q_B-reconstituted reaction centers. Conditions: 100 mM NaCl, 0.05% LDAO, 20 μM Q-10, 100 μM ferrocene, 0.6 mM potassium ferrocyanide; spectrophotometric assay with various pH indicators. ○, internal calibration with average $H^+/P^+ = 1.0$; ●, external calibration with standard HCl. - - - - -, line taken from Fig. 5A, i.e., fitted to data in 0.03% Triton X-100.

X-100 as the solubilizing agent. In both detergents, the proton stoichiometry appears to fall at pH values below 7, and in Triton there is some indication that it increases again after reaching a minimum between pH 6 and 6.5. This potentially interesting region could not be adequately probed in LDAO, as the detergent induced large, positive shifts in the pKs of the indicators, leaving none with sufficient sensitivity to use at pH values much below 7.

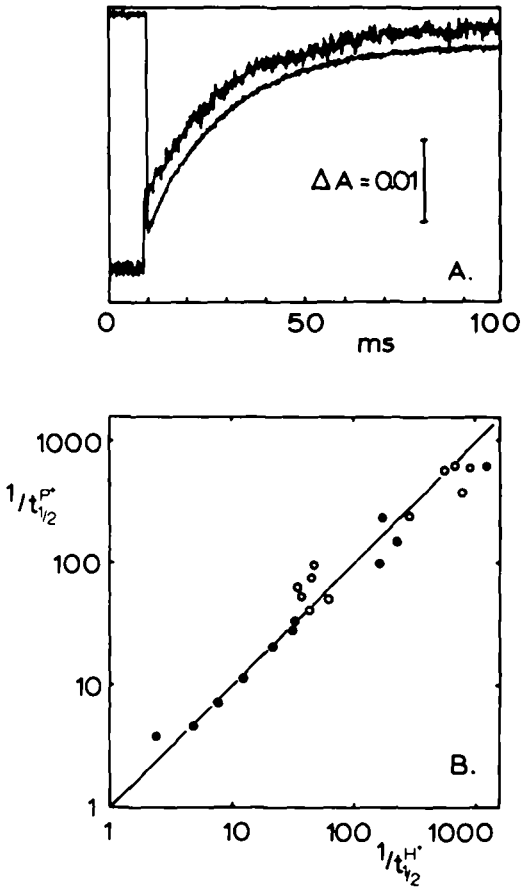

Fig. 7. Kinetic correlation between P^+ rereduction and the extra proton uptake in the presence of exogenous donor. (A) Parallel measurements of the P^+ absorbance change at 430 nm (downward deflection at the flash), and net proton binding, measured at 586 nm (upward deflection). Conditions: 1.05 μM reaction centers (R26), 100 mM NaCl (pH 6.3), 0.03% Triton X-100, 20 μM Q-10, 60 μM terbutryn, 10 μM ferrocene, 0.5 mM potassium ferrocyanide, 40 μM chlorophenol red. (B) Compiled data of parallel P^+ and H^+ kinetic measurements, with (○) and without (●) 60 μM terbutryn. Conditions: 100 mM NaCl, 0.03% Triton X-100, 20 μM Q-10 (pH = 6.4–8.0).

Kinetic correlation between P^+-rereduction and first flash proton binding

It is clear from the data of Fig. 5, that the observed, flash-induced proton-binding behavior is a complex function of the various states of the RC. Although prior knowledge of the equilibrium redox properties of the primary donor and the acceptor quinones leads us to expect almost exclusive control of the proton uptake by the redox state of the quinones, our observations suggest that the primary donor makes an unexpectedly large contribution. Proof that this influence arises largely from the redox state of P^+/P, rather than the presence of an exogenous, secondary donor, per se, is shown in Fig. 7A, which shows simultaneous measurements of P^+-rereduction and H^+ binding by RCs, in the presence of donor and terbutryn. The fast phase of proton binding is equivalent to that seen in the absence of donor; the slow phase correlates well with the P^+-reduction. Fig. 7B compiles many such measurements for both Q_B-reconstituted and terbutryn-inhibited RCs.

It may be noted, in Fig. 1B, that there is no indication that the proton binding on the first flash is preceded by proton release. This was also remarked, previously, for RCs in the absence of exogenous donor [1].

Discussion

In the previous article, the failure of the flash-induced reaction center states, $P^+Q_A^-$ and $P^+Q_B^-$, to bind protons at low pH, was described [1]. This anomalous behavior was accounted for by a model in which the functional groups responsible for the H^+ uptake were under the simultaneous influence of the redox states of the acceptor quinones and the primary donor, such that the differences in pK before and after flash activation were quite small (0.1–1.5 pH units). The possibility that uptake to the semiquinone was masked by an independent proton release from the P^+/P couple [26] was rendered unlikely by the failure to detect a transient H^+ release prior to binding (Ref. 1, see also Fig. 1B). Thus, the H^+ binding is a response to the net redox state of the RC redox couples, P^+/P and Q/Q^-. Nevertheless, the separate influences of Q/Q^- and P^+/P has been revealed, in

this work, by the use of exogenous donors to rereduce P^+ and produce the state PQ^-.

The net proton binding associated with a redox transition arises from pK shifts induced by the redox state change of the RC. In the flash induced transition, $PQ \rightarrow P^+Q^-$, the charge separation state has multiple effects on several ionizable groups. Similarly, the flash-induced proton binding observed in the presence of donors reflects the protonation behavior of the same groups in the transition $PQ \rightarrow PQ^-$. By adding the protonation equilibria for the P^+Q state, a scheme is completed that can interpret the proton binding data for all three acceptor quinone configurations (Q_A, Q_A/ + terbutryn and Q_B), in the presence and absence of donors, as well as predicting other aspects of reaction center behavior (Fig. 8A). Four protonatable groups are envisioned, with pK values that depend on the redox states of the primary donor and acceptor quinones, as well as the occupancy of the Q_B-binding site. Each column of protonation states corresponds to a different redox state of the reaction center components, and the redox states are functionally related to each other as described in Fig. 8B. It is presumed that there is no obligatory sequence to the protonation events, i.e., no ordered addition, in which case the four protonatable groups in each RC state should contribute to a fully connected network of equilibria. For clarity, however, a linear sequence of five protonation states is shown.

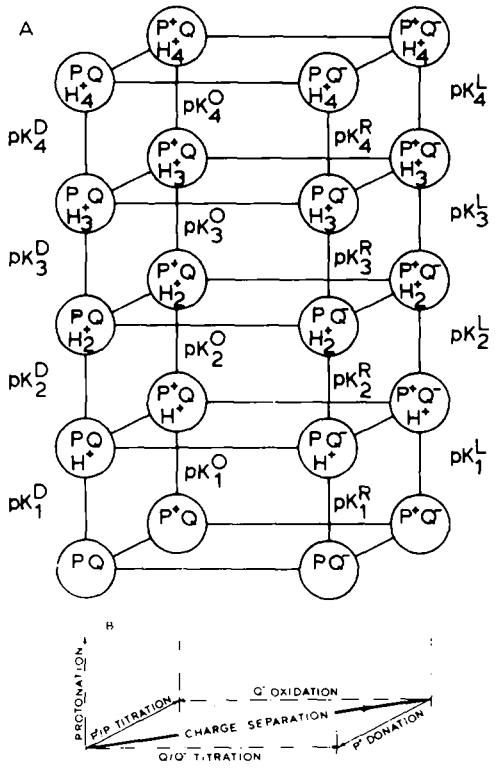

Fig. 8. Redox-linked protonation equilibria in reaction centers. (A) Scheme for four protonatable groups under the simultaneous influences of Q/Q^- and P^+/P. Each vertical column represents a single redox state of the RC, indicated by superscripts on the pKs: D, dark adapted (PQ), L, light activated (P^+Q^-), O, oxidized (P^+Q), R, reduced (PQ^-). The linear sequences in each column are a simplification of the fully connected networks of equilibria expected for independent protonation events. (B) Key for the functional transitions between the redox states of part A.

For four protonatable groups, as shown in Fig. 8A, the net H^+ uptake, accompanying a redox-state transition, is given by the sum of four overlapping, bell-shaped curves, according to:

$$H^+/P^+ = \sum_{i=1}^{i=4}\left(\frac{10^{pK_i^A - pH}}{1+10^{pK_i^A - pH}} - \frac{10^{pK_i^B - pH}}{1+10^{pK_i^B - pH}}\right) \qquad (1)$$

where pK_i^B and pK_i^A are the pK values of the ith group before (B) and after (A) the transition, respectively. Four different redox states of the RC are considered: PQ (superscript D, dark-adapted), P^+Q^- (L, light-activated), PQ^- (R, reduced) and P^+Q (O, oxidized). Each pair of terms in Eqn. 1 describes the net proton binding by a single group. 4 is the minimum number of groups that can satisfactorily account for the proton binding in the presence of donor and, for consistency, the same number has been used for the data obtained in the absence of donor [1]. The various pK values, which are listed in Table II, were obtained by first fitting each data set separately. Values for pK_i^L and pK_i^R were then refined to obtain best visual fits for proton binding to P^+Q^- and to PQ^-, using the same set of averaged, dark pK values (pK_i^D) for both. Clearly the same initial (dark) state (PQ) is involved in both transitions. The values for pK_i^O were determined only through the application of detailed balance, i.e., the sum of free energies around a cycle is zero.

TABLE II

pK VALUES FOR THE SCHEME OF FIG. 8A, DERIVED FROM FIG. 5A–C

$i = 1$–4 are the group numbers.

	Q_B				Q_A/+terbutryn				Q_A			
	$i=1$	$i=2$	$i=3$	$i=4$	$i=1$	$i=2$	$i=3$	$i=4$	$i=1$	$i=2$	$i=3$	$i=4$
RC state/pK												
PQ pK^D	9.1	8.1	6.4	4.5	9.7	8.35	6.8	4.8	9.2	8.35	6.9	5.3
P^+Q^- pK^L	10.6	8.7	6.85	4.8	10.5	8.6	6.9	4.9	9.65	8.65	7.1	5.4
PQ^- pK^R	10.65	9.1	7.95	6.0	10.55	8.65	7.4	5.9	9.65	8.65	7.4	6.2
P^+Q pK^O	9.05	7.7	5.3	3.3	9.65	8.3	6.3	3.8	9.2	8.35	6.6	4.5
$\Delta pK(P^+)$	−0.05	−0.4	−1.1	−1.1	−0.05	−0.05	−0.5	−1.0	0	0	−0.3	−0.8
$\Delta pK(Q^-)$	1.55	1.0	1.55	1.5	0.85	0.3	0.6	1.1	0.45	0.3	0.5	0.9

Table II also shows the effect (ΔpK) of the individual redox couples, P^+/P and Q/Q^-, on each of the four protonation steps. It is clear that P^+/P has almost no effect on the highest pK, which is traditionally associated with the Q/Q^- redox couple, and only in Q_B-reconstituted RCs does it have some effect on the second-highest pK. The two lower pK processes, on the other hand, are significantly influenced by P^+/P. The lowest pK region is the least well characterized, due to the absence of extensive data in the absence of donors, below pH 6.5. However, preliminary data by McPherson et al. [27], on Q_B-depleted RCs, show good general agreement with ours, with more extensive low pH data, down to pH 4.5. It is the sensitivity of the lower pK values to P^+/P that is largely responsible for the suppression of proton binding at low pH, in the absence of donor, and its partial recovery in the presence of donor.

The influence of Q^- is felt on all protonation steps. It is most acute for the high pK transitions, with Q_B^- having the largest effect ($\Delta pK = 1.55$), and Q_A^-, in the absence of any occupation of the Q_B site, the smallest ($\Delta pK = 0.25$).

A particularly striking prediction of the scheme of Fig. 8A is the possibility of H^+ release from reaction centers. From the pK assignments made for the PQ, P^+Q^- and PQ^- states, the pK values for the P^+Q state (pK_i^O) can be obtained. These predict the occurrence of proton release in the $PQ \rightarrow P^+Q$ transition, especially at low pH, where Table II indicates P^+/P to have its largest influence on pK values. We have previously reported that ferricyanide, at low pH, can be a surprisingly effective oxidant of the acceptor semiquinones, acting through Q_A^- [24]. Thus, we can expect the following sequence of events:

$$PQ \overset{H^+}{\underset{pK^D\,(H^+)_D}{\longleftrightarrow}} PQ \overset{h\nu}{\Longrightarrow} \underset{(H^+)_D}{P^+Q^-} \overset{H^+}{\underset{(H^+)_L}{\longleftrightarrow}} P^+Q^- \xrightarrow[\text{ferro}]{\text{ferri}} \underset{(H^+)_L}{P^+Q} \overset{H^+}{\underset{(H^+)_O\,pK^O}{\longleftrightarrow}} P^+Q$$

The subscripts to the bound H^+ indicate the continuing adjustment of the RC protonation state to the sequence of redox states, following the flash. The net proton binding or release, however, is determined only by the pK values of the initial and final states, pK^D and pK^O. The results, for RCs in the presence of terbutryn, are shown in Fig. 9. The immediate response, after a flash, is a small amount of proton binding, as we expect from our studies in the absence of donors to P^+ [1]. Following this, there is a progressive H^+ release which exhibits the same kinetics as the P^+ decay. Under these conditions, the charge separation state, P^+Q^-, disappears via two routes: the normal charge recombination, which is accompanied by reversal of the flash-induced proton binding, and oxidation of Q^- by ferricyanide, which leaves a 'trapped' P^+ that decays very slowly via reduction by exogenous donors, e.g., ferrocyanide. By the end of the fast decay of P^+, there

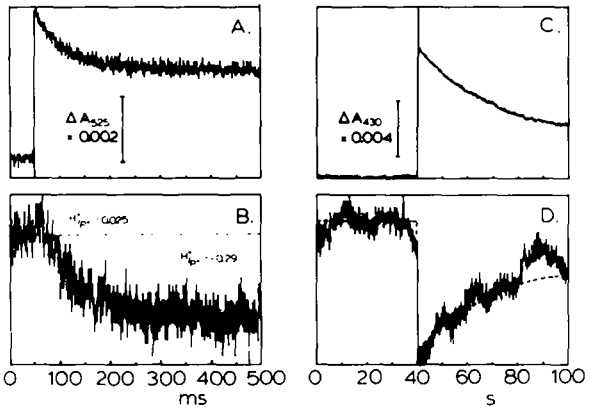

Fig. 9. Net proton release associated with primary donor oxidation: $PQ \rightarrow P^+Q$. Conditions: 1.1 μM reaction centers (R26), 100 mM NaCl (pH 5.94), 0.03% Triton X-100, 20 μM Q-10, 60 μM terbutryn, 250 μM potassium ferricyanide, 40 μM bromocresol purple. Left panels: Simultaneous measurements of (A) P^+ absorbance changes, at 525 nm (isosbestic for the pH indicator), and (B) net proton binding/release, at 585 nm (isosbestic for PQ/P^+Q^-). Right panels: Separate measurements of (C) slow kinetics of P^+ rereduction (plus 10 mM Mes), at 430 nm, and (D) proton rebinding at 585 nm. - - - - - -, Inverted P^+ trace, from part (C). Note different time scales in left and right panels.

is a net proton release which is determined by the protonation properties of the new reaction center state, P^+Q. Since only a portion of the RCs are trapped in this form, the H^+/P^+ stoichiometry is calculated on the basis of the remaining P^+, rather than on the total reaction center concentration. In the presence of terbutryn, the measured proton release was 0.29 H^+/P^+ compared to a value of 0.25, predicted from the pK values in Table II. For Q_B-reconstituted RCs, the observed stoichiometry* of H^+ release was 0.37 H^+/P^+ [26], and the calculated value was 0.56. We consider the observed values to be in reasonably good agreement with those expected on the basis of the scheme of Fig. 8, especially in view of the greater uncertainties associated with the lower pK values.

The influence of P^+/P on the lower pK values is also seen in the kinetics of proton binding. The additional H^+-uptake seen in the presence of donor, compared to the absence, occurs with kinetics that match the rereduction of P^+. This correlation is established in Fig. 7, over a wide time range, both for Q_B-reconstituted and for terbutryn-inhibited RCs.

For all the wealth of data that apparently resides in Table II, it is not a simple matter, at this time, to associate the functional pKs with amino acid residues in the RC proteins. Nevertheless, some speculation is possible for the highest pK group, which responds in a suggestive fashion to the redox states of the two quinones and to the occupant of the Q_B binding site, i.e., ubiquinone, terbutryn or nothing. The value for pK_1^P, corresponding to a pK on the oxidized form of the acceptor quinones, is very similar for both Q_B-depleted and Q_B-reconstituted RCs, but is shifted 0.5 pH units in the presence of terbutryn. The value of pK_1^L, on the other hand, is almost the same for Q_A^-(+terbutryn) and for Q_B^-. The X-ray structural analysis of the RC from *Rhodopseudomonas viridis* [28] shows that terbutryn binds in the Q_B pocket, at the opposite end from the iron-histidine complex, probably forming strong hydrogen bonds to a serine (residue 223 in the L subunit), adjacent to a tyrosine (L222). In both *Rps. viridis* [29] and *Rb. sphaeroides* [10,30], the secondary quinone itself binds rather weakly, and much of the binding affinity in isolated RCs is provided by the entropic effect of the hydrophobic tail [6,31]. For Q_A, comparative binding studies of many different quinones and quinone analogs suggest that only one of the carbonyl oxygens contributes a significant binding energy [32] and this is consistent with the *Rps. viridis* X-ray structural data, which shows it clearly H-bonded only through the carbonyl furthest from the iron-histidine complex [28]. The more recent X-ray structure for the *Rb. sphaeroides* reaction center shows Q_B also to be asymmetrically coordinated, but with the stronger H-bond at the iron-histidine end (Refs. 33 and 34; see also Schiffer, M., personal communication). On the other hand, the semiquinone of Q_B binds extremely strongly [35], and ENDOR studies on the Q_A^- and Q_B^- states, In *Rb. sphaeroides,* indicate that the semiquinones form strong hydrogen bonds through both quinone oxygens [36].

On the basis of these data, we considered that

* The stoichiometries quoted in the earlier work (Ref. 26) were based on an erroneous extinction coefficient for P^+/P at 430 nm, and should be diminished by 20%.

the highest pKs associated with proton binding, and with the redox titrations of Q_A, might reflect the protonation of serine (L223). However, a herbicide-resistant mutant of *Rb. sphaeroides,* which has been identified as a serine-to-proline mutation, at L223 [37], apparently exhibits the same pH dependence as the wild type, for the one-electron transfer equilibrium between $Q_A^- Q_B$ and $Q_A Q_B^-$ (Okamura, M.Y., personal communication). Since this equilibrium is believed to involve the same protonation states as the proton uptake, this renders the assignment of serine (L223) unlikely, and turns our attention elsewhere, including the adjacent tyrosine (L222). Indeed, the possible involvement of this residue in protonation events, associated with Q_B^-, has been raised before [37]. It lies against the back of the peptide chain surrounding the Q_B pocket. Although it is quite close to the surface, tyrosine L222 is oriented away from the aqueous interface and is hydrogen bonded to the carbonyloxygen of residue M43, a glycine residue in the M subunit (Schiffer, M., personal communication). Both the L and the M subunits contribute to the iron-binding region, which provides a strong focal point for the acceptor-quinone complex. The interaction between the two subunits provided by the tyrosine-peptide carbonyl hydrogen bond may also assist in

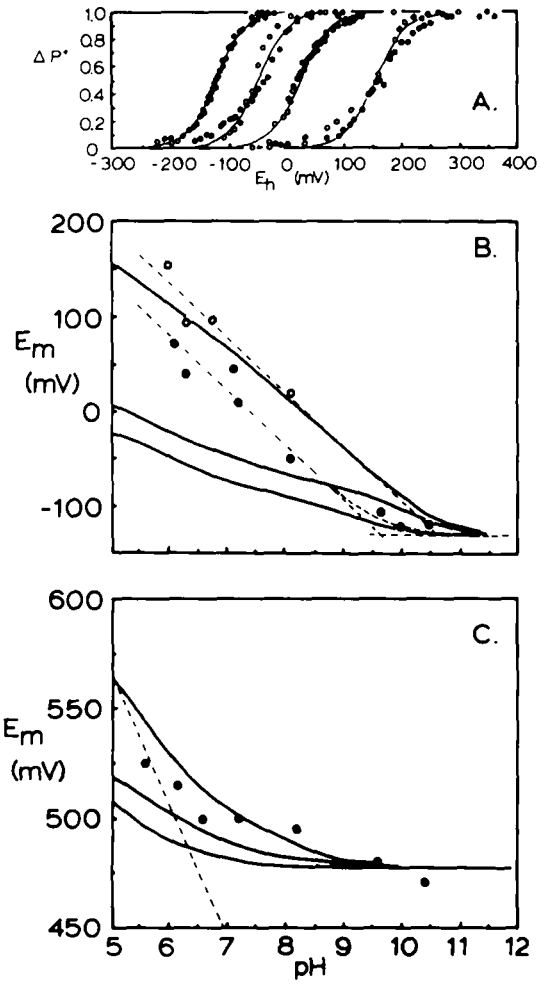

Fig. 10. Predicted and experimental redox midpoint potentials for primary donor and acceptor quinones. (A) Redox titrations of Q_A/Q_A^- assayed by the flash-induced production of P^+, measured at 430 nm: oxidative (○) and reductive (●) titrations. From right to left: plus 20 μM Q-10 and 60 μM terbutryn (pH 6.0); the same (pH 8.1); with Q-10 only (no terbutryn) (pH 8.1); the same (pH 10.0). (B) $E_m(Q/Q^-)$ vs. pH. Experimental determinations of $E_m(Q_A/Q_A^-)$: ●, with 20 μM Q-10; ○, with 60 μM terbutryn. Solid lines: computed curves for $E_m(Q_B/Q_B^-)$ in Q_B-reconstituted reaction centers (top), and for $E_m(Q_A/Q_A^-)$ in the presence of terbutryn (middle) and in Q_B-depleted reaction centers (bottom), calculated from the pK_i^D and pK_i^R values given in Table II, using the equation:

$$E_m = E_m^0 + 59 \log \frac{\prod_i (1 + 10^{pK_i^R - pH})}{\prod_i (1 + 10^{pK_i^D - pH})} \text{ mV.}$$

E_m^0 is the limiting midpoint potential at high pH, above the highest pK of the reduced species. E_m^0 was set at -130 mV, for all simulations, to give the best coincidence of calculated and experimental values of $E_m(Q_A/Q_A^-)$ at high pH, and in accordance with $K_2 \approx 1$ at high pH (see Fig. 11). Dashed lines: these are drawn through the data points to indicate the pH dependences expected for a single protonatable group (slope = −58 mV/pH), with a pK^R of 9.6 (lower line) or 10.5 (upper line). (The coincidence between the simulated (solid) curve for $E_m(Q_B/Q_B^-)$ and the data for $E_m(Q_A/Q_A^-)$ in the presence of terbutryn, is accidental). (C) $E_m(P^+/P)$ vs. pH. Experimental determinations of $E_m(P^+/P)$: , with 20 μM Q-10. Solid lines: computed curves for $E_m(P^+/P)$ in the presence of 20 μM Q-10 (Q_B-reconstituted RCs) (top), in the presence of 60 μM terbutryn (middle) and in Q_B-depleted RCs (bottom), calculated from the pK_i^D and pK_i^O values in Table II, as described for $E_m(Q/Q^-)$ in part A, with $E_m^0(P^+/P) = 475$ mV. Dashed line: theoretical line for a single protonatable group on the reduced form, slope = −58 mV/pH.

the functional communication between the Q_A and Q_B binding sites implied in this model. Such mutual influences are clearly indicated by the effects that terbutryn and ubiquinol binding, to the Q_B site, have on the E_m of Q_A [5].

From the protonation equilibria outlined in Fig. 8A, it should be possible to determine the pH dependences of the redox properties of the primary donor and the acceptor quinones, as well as the pH dependence of the electron-transfer equilibrium between Q_A and Q_B. These are shown in Figs. 10 and 11, together with experimental data where available. The derived pK values for the PQ and P^+Q states imply a weak average pH dependence of $E_m(P^+/P)$, that is quite consistent with data in the literature [3,38], and with our own measurements, which reveal an average slope of about -14 mV/pH unit (Fig. 10C). The calculated values show that the expected influence of the acceptor side on $E_m(P^+/P)$ is mild in the experimentally accessible pH range.

The pH dependences for the acceptor quinone couples are shown in Fig. 10B. The net H^+ binding for PQ_B^- implies a substantial pH dependence for the Q_B/Q_B^- redox couple, which is consistent with determinations made in chromatophores [4]. The net H^+-binding observed for the PQ_A^- and PQ_A^-(+terbutryn) states, however, are much smaller and predict rather weak pH dependences for the Q_A/Q_A^- redox couple, in marked contrast to the equilibrium behavior in chromatophores [3], or in isolated RCs in phospholipid vesicles [5]. We, therefore, undertook some equilibrium redox titrations of Q_A/Q_A^- in isolated RCs in Triton. This proved to be difficult, as we have noted previously [5], because equilibrium could not be established in the absence of certain redox mediators, notably the phenazines, which, when present in normal mediator concentrations, were so reactive as to interfere with the assay method (measurement of flash-induced P^+). By using very low concentrations of PMS and PES (up to 1 μM), we were able to obtain reasonably reversible titrations (Fig. 10A). The pH dependence of $E_m(Q_A/Q_A^-)$, in the presence and absence of terbutryn, is shown in Fig. 10B. It is evidently similar to that reported for chromatophores and for RCs in phospholipid vesicles. This leaves a clear discrepancy between the proton

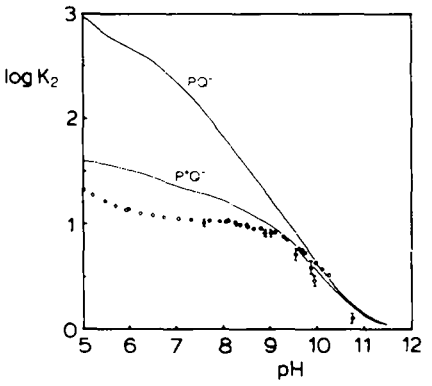

Fig. 11. Measured and predicted values for the one-electron equilibrium (K_2): $Q_A^- Q_B \leftrightarrow Q_A Q_B^-$. Lines are drawn according to the model described in the text and the pK values given in Table II, using the equation: $\Delta E_m = E_m(Q_B/Q_B^-) - E_m(Q_A/Q_A^-) = 59 \log K_2$ mV. $E_m(Q_A/Q_A^-)$ and $E_m(Q_B/Q_B^-)$ were calculated as described for Fig. 10. ○, experimental values of K_2 determined from the recombination kinetics, in the absence of exogenous donor, calculated according to Ref. 10: $t_{1/2}(P^+Q_B^-) = t_{1/2}(P^+Q_A^-)[1+K_2]$, where $t_{1/2}(P^+Q_B^-)$ nd $t_{1/2}(P^+Q_A^-)$ are the half-times for recombination in the presence and absence of functional Q_B. $t_{1/2}(P^+Q_A^-)$ was taken as 65 ms, pH independent, throughout (Refs. 11 and 12, but see footnote, p. 345.

uptake data – or its analysis – and the equilibrium redox titrations of Q_A. However, there are previous reports of pH independence for $E_m(Q_A/Q_A^-)$, in Triton as well as in vesicles [5,39], one of which was performed by ESR assay of the $g = 1.82$ signal of Q_A^- [39]. The dense samples used in ESR measurements and, consequently, the high concentrations of mediators, greatly facilitate the achievement of redox equilibrium. Furthermore, the assay is performed in the dark and does not suffer from the kinetic interference encountered with reactive mediators. Thus, in spite of the difficulties associated with the proton measurements, at the present time we have more confidence in them than in the redox titrations.

However, if we accept the redox titrations as the source of the discrepancy between the PQ_A^- proton binding and redox data, we are then faced with another discrepancy when we calculate the electron-transfer equilibrium (K_2) between $Q_A^- Q_B$ and $Q_A Q_B^-$ from the PQ_A^- and PQ_B^- proton binding data. This equilibrium has been shown to be roughly pH independent, below about pH 9, by two methods [2,10–12,16] – the back reaction

kinetics for $P^+Q_AQ_B^-$, which proceeds via equilibrium with $P^+Q_A^-Q_B$ and recombination from that state, and the extent of cytochrome oxidation in a flash series in which the presence of Q_A^- causes less turnover on the second and subsequent flashes compared to the first. The fact that these two methods of determination agree implies that the redox state of P^+/P does not significantly affect the $Q_A^-Q_B/Q_AQ_B^-$ equilibrium. When K_2 is calculated from the proton-binding measurements, agreement is obtained between the value of K_2 determined from the P^+Q^- proton binding and from the P^+Q^- back reaction data (Fig. 11) *, but the PQ^- proton binding data predict a significant pH-dependence for the equilibrium, reflecting the much greater net proton binding by PQ_B^- compared to PQ_A^-. At the present time we cannot resolve these discrepancies which are under further investigation.

Conclusions

The present study only partially reproduces our original observations on the proton binding stoichiometry of reaction centers in the presence of secondary acceptor (Q_B) and donor [2]. However, there are at least two possible explanations for the discrepancies, if we accept that the earlier experimental conditions were reported erroneously. Thus, if the baseline subtracted was that obtained with no dye, rather than with dye and buffer, then a substantial oscillation could be imposed on the apparent proton binding, due to the electrochromic response of bound dye molecules. Alternatively, if the external calibration was in error, then the deeper oscillations reported at that time could indicate significant proton release from the donor side reactions. Although cytochrome *c* was the intended donor, 10–20 μM DAD was also present to aid in poising the redox potential of the sample. This could also account for the enhancement of the oscillations at low pH (less than 6.5) if the proton release stoichiometry of DAD oxidation also increases at low pH. This is supported by our observations on the steady-state stoichiometry of proton binding in a flash train (Fig. 4C), but it is not consistent with the redox properties of the fully reduced/fully oxidized couple, as determined by Prince et al. [21] using polarographic methods. The difference may reflect the properties of the semiquinone of DAD which, in our experience, is the most actively donating species. The semiquinone state was not characterized in the polarographic study.

We conclude, on the basis of our current work, that at least four groups are involved in the flash-induced proton uptake by isolated RCs. Furthermore, although these groups can best be assigned, functionally, to the acceptor quinone complex, the presence of a donor to P^+ dramatically changes the observed proton binding of photoactivated reaction centers. This is summarized in Fig. 8A, which is adequate to account for the observed proton binding for a variety of acceptor quinone configurations, in the presence or absence of donors. When Q_B is functional, hydrogen ion uptake in the presence of donor approaches what is expected from the redox properties of the secondary quinone, i.e., approximately 1 H^+/e^+. The failure to observe proton binding at pH values below 9, in the absence of donor, arises from the existence of a second pK, when the quinone is oxidized. In fact, the decline in proton uptake as the pH is lowered implicates at least four distinguishable groups, each with distinct pK values for the oxidized and reduced forms of the acceptor quinones. The rather different proton binding data seen for Q_A-active and Q_B-active RCs, reflect differences in the pK values associated with Q_A and Q_B, and the influence of terbutryn.

The rereduction of P^+ by donors causes changes in the pK values of some of the groups. The pK shifts induced by P^+/P are largest for the low pK groups, giving rise to a substantial change in the net proton binding observed at low pH. In the case of Q_B-reconstituted RCs, the net proton binding at pH 7.5, for example, increases from about 0.25 H^+/P^+, in the absence of donor, to 0.9 H^+/P^+ in the presence of donor. The resulting net

* A recent report by McPherson et al. (Ref. 42) describes a weak pH dependence for the $P^+Q_A^-$ back reaction in isolated RCs. The rate increased by about 40% as the pH was raised from pH 6.5 to pH 11, apparently reflecting electrostatic effects associated with the H^+ binding. Such a pH-dependence would substantially improve the fit, in Fig. 11, between the measured and calculated values for K_2 in the P^+Q^- state, especially below pH 9.

H^+ binding for PQ_B^- implies a substantial pH dependence for the Q_B/Q_B^- redox couple. This is consistent with redox determinations made in chromatophores [4]. The net H^+ binding observed for the PQ_A^- and PQ_A^-(+terbutryn) states, however, are much smaller and predict rather weak pH dependences for the Q_A/Q_A^- redox couple, in marked contrast to the equilibrium behavior in chromatophores [3], or for isolated RCs in phospholipid vesicles [5] and in detergent (this work). This discrepancy is still unsettled, but the −58 mV/pH dependence of this couple in chromatophores seems to be rather well established over a wide pH range, upto the pK on the reduced form [3]. This may indicate substantial masking, or burying, of ionizable groups by the membrane environment, such that the electrostatic influences of the Q_A/Q_A^- redox states are focussed on a single group.

By virtue of the principle of detailed balance, any variations in the effect of P^+/P on pK values associated with the Q/Q^- redox couples will be reciprocated as changes in pK values for the P^+/P redox couple, linked to the status of the acceptor quinone complex. Only in the case of *Chromatium* has the E_m of P^+/P been explicitly considered as exhibiting a pH dependence [38]. More generally, it has been implicitly considered to be pH independent [3] but, as shown in this work, for *Rb. sphaeroides* it actually exhibits an average slope of −12 to −16 mV/pH, and a similar dependence is encountered in *Rhodopseudomonas viridis* (Shopes, R.J., Gao, J. and Wraight, C.A., unpublished observations). This pH dependence is sufficient to encompass the pK values implied by our description of the proton binding behavior, and the predictions of the scheme of Fig. 8A appear to be satisfactorily borne out here.

The notion of linked pK changes between the primary donor, P, and the acceptor quinones, raised the interesting possibility that the RC might act as a proton pump, in much the same way as has been shown for cytochrome oxidase of mitochondria [40] and bacteriorhodopsin of *Halobacterium halobium* [41]. However, our failure to observe transient H^+ release followed by rebinding does not support this suggestion. Furthermore, preliminary measurements on RCs incorporated into phospholipid vesicles, have not revealed any vectorial movement of protons. At the present time, therefore, we consider that all the protolytic reactions, involved in the observed proton uptake by RCs, most likely occur on the same side of the membrane, i.e., the acceptor side.

Acknowledgements

This work was supported by the National Science Foundation through grants (PCM 80-12032, PCM 83-16487 and DMB 86-17144) to C.A.W.

References

1 Maróti, P. and Wraight, C.A. (1988) Biochim. Biophys. Acta 934, 314–328.
2 Wraight, C.A. (1979) Biochim. Biophys. Acta 548, 309–327.
3 Prince, R.C. and Dutton, P.L. (1978) in The Photosynthetic Bacteria (Clayton, R.K. and Sistrom, W.R., eds.), pp. 439–453, Plenum Press, New York.
4 Rutherford, A.W. and Evans, M.C.W. (1980) FEBS Lett. 110, 257–261.
5 Wraight, C.A. (1981) Isr. J. Chem. 21, 348–354.
6 Wraight, C.A., Stein, R.R., Shopes, R.J. and McComb, J.C. (1984) in Advances in Photosynthesis Research (Sybesma, C., ed.), Vol. I, pp. 629–636, Martinus Nijhoff/Dr. W. Junk Publishers, Dordrecht.
7 Brandt, K.G., Parks, P.C., Czerlinski, G.H. and Hess, G.P. (1966) J. Biol. Chem. 241, 4180–4185.
8 Davis, L.A., Schejter, A. and Hess, G.P. (1974) J. Biol. Chem. 249, 2624–2632.
9 Czerlinski, G.H. and Dar, K. (1971) Biochim. Biophys. Acta 234, 57–61.
10 Wraight, C.A. and Stein, R.R. (1983) in The Oxygen Evolving System of Photosynthesis (Inoue, Y. et al., eds.), pp. 383–392, Academic Press, Japan, Tokyo.
11 Kleinfeld, D., Okamura, M.Y. and Feher, G. (1984) Biochim. Biophys. Acta 766, 126–140.
12 Stein, R.R. (1985) Ph.D. Thesis, University of Illinois, Urbana, IL.
13 Prince, R.C., Dutton, P.L. and Bruce, J.M. (1983) FEBS Lett. 160, 273–276.
14 Fujihara, Y., Kuwana, T. and Hartzell, C.R. (1974) Biochim. Biophys. Res. Commun. 61, 538–543.
15 Kleinfeld, D., Okamura, M.Y. and Feher, G. (1985) Biochim. Biophys. Acta 809, 291–310.
16 Wraight, C.A. and Stein, R.R. (1980) FEBS Lett. 113, 73–77.
17 Verméglio, A. (1977) Biochim. Biophys. Acta 459, 516–524.
18 Petty, K.M. and Dutton, P.L. (1976) Arch. Biochem. Biophys. 172, 335–345.
19 Junge, W. and Ausländer, W. (1973) Biochim. Biophys. Acta 333, 59–70.
20 Saphon, S. and Crofts, A.R. (1977) Z. Naturforsch. 32c, 810–816.

21 Prince, R.C., Linkletter, S. and Dutton, P.L. (1981) Biochim. Biophys. Acta 635, 132–148.
22 Meyer, T.J. and Taube, H. (1968) Inorg. Chem. 7, 2369–2379.
23 Lim, H.S., Barclay, D.J. and Anson, F.C. (1972) Inorg. Chem. 11, 1460–1466.
24 Shopes, R.J. and Wraight, C.A. (1986) Biochim. Biophys. Acta 848, 364–371.
25 Agalidis, I. and Velthuys, B. (1986) FEBS Lett. 197, 263–266.
26 Maróti, P. and Wraight, C.A. (1987) in Progress in Photosynthesis Research (Biggins, J., ed.), Vol. II, pp. 401–404, Martinus Nijhoff, Dordrecht.
27 McPherson, P., Okamura, M.Y. and Feher, G. (1987) Biophys. J. 51, 125a.
28 Michel, H., Epp, O. and Deisenhofer, J. (1986) EMBO J. 5, 2445–2451.
29 Shopes, R.J. and Wraight, C.A. (1985) Biochim. Biophys. Acta 806, 348–356.
30 Okamura, M.Y., Isaacson, R.A. and Feher, G. (1975) Proc. Natl. Acad. Sci. USA 72, 3491–3495.
31 McComb, J.C. (1987) Ph.D. Thesis, University of Illinois, Urbana, IL.
32 Gunner, M.R., Braun, B.S., Bruce, J.M. and Dutton, P.L. (1985) in Antennas and Reaction Centers of Photosynthetic Bacteria (Michel-Bayerle, M.E., ed.), pp. 298–305, Springer-Verlag, Berlin.
33 Chang, C.-H., Tiede, D.M., Tang, J., Norris, J.R. and Schiffer, M. (1986) FEBS Lett. 205, 82–86.
34 Allen, J.P., Feher, G., Yeates, T.O., Komiya, H. and Rees, D.C. (1987) Proc. Natl. Acad. Sci. USA 84, 5730–5734.
35 Crofts, A.R. and Wraight, C.A. (1983) Biochim. Biophys. Acta 726, 149–185.
36 Lubitz, W., Abresch, E.C., Debus, R.J., Isaacson, R.A., Okamura, M.Y. and Feher, G. (1985) Biochim. Biophys. Acta 808, 464–469.
37 Paddock, M.L., Williams, J.C., Rongey, S.H., Abresch, E.C., Feher, G. and Okamura, M.Y. (1987) in Progress in Photosynthesis Research (Biggins, J., ed.), Vol. III, pp. 775–778, Martinus Nijhoff, Dordrecht.
38 Case, G.D. and Parson, W.W. (1971) Biochim. Biophys. Acta 253, 187–202.
39 Dutton, P.L., Leigh, J.S. and Wraight, C.A. (1973) FEBS Lett. 36, 169–173.
40 Wikström, M. and Kraab, K. (1979) Biochim. Biophys. Acta 549, 177–222.
41 Stoeckenius, W., Lozier, R. and Bogomolni, R.A. (1979) Biochim. Biophys. Acta 505, 215–278.
42 McPherson, P., Arno, T., Okamura, M.Y. and Feher, G. (1988) Biophys. J. 53, 271a.